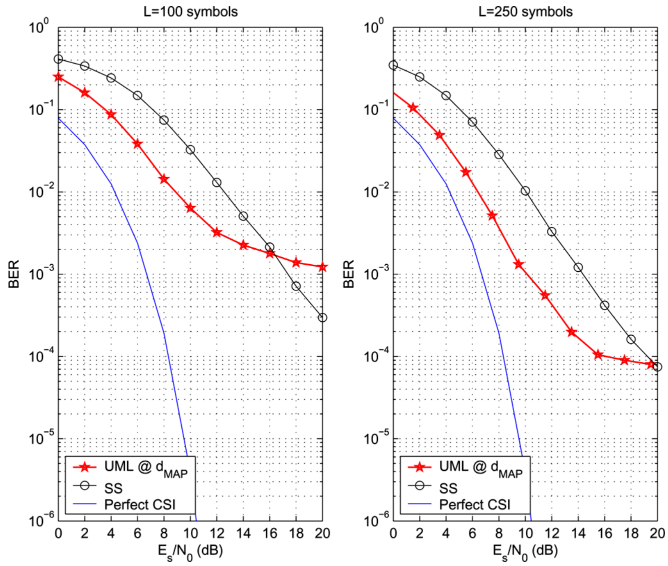

Fig. 4. BER for the MMSE detector as a function of E_s/N_0.

when using the proposed method compared to the case with perfect channel state information (CSI). However this E_s/N_0 loss reduces to just 2 dB with $L = 250$ symbols. In that case, the proposed method also provides a BER that is one order of magnitude lower than that provided by the SS scheme.

VI. Conclusion

A closed-form waveform estimation technique has been proposed based on the low-SNR UML criterion. By introducing a signal subspace constraint and the vec operator, the nonlinear optimization problem is converted into a least-squares problem on the second-order statistics of the received signal. The proposed subspace-compressed approach can be seen as a principal component analysis, and thus, a reduction in the computational burden is obtained through a tradeoff between bias and variance. Moreover, the subspace constraint restricts the solution space and hence, it avoids many of the effects of ill-conditioning and local-maxima of traditional ML channel estimators. Simulation results show the superior performance of the proposed technique with respect to other closed-form methods based on second-order statistics.

References

[1] G. Vázquez and J. Riba, "Non-data-aided digital synchronization," in *Signal Processing Advances in Wireless and Mobile Communications*. Englewood Cliffs, NJ: Prentice-Hall, 2000, vol. 2, ch. 9.
[2] L. Yang and G. B. Giannakis, "Ultra-wideband communications: An idea whose time has come," *IEEE Signal Process. Mag.*, vol. 21, no. 6, pp. 26–54, Nov. 2004.
[3] R. T. Hoctor and H. W. Tomlinson, G. E. Research and Development Center, "An overview of delay-hopped, transmitted-reference RF communications," Jan. 2002, pp. 1–29.
[4] L. L. Scharf and D. W. Tufts, "Rank reduction for signal modelling and parameter estimation," in *Proc. 20th Asilomar Conf. Signals, Syst. Comput.*, 1986, pp. 467–471.
[5] C. J. L. Martret and G. B. Giannakis, "All-digital PAM impulse radio for multiple-access through frequency-selective multipath," in *Proc. IEEE GLOBECOM*, Nov.—Dec. 2000, vol. 1, pp. 77–81.
[6] B. Ottersten, M. Viberg, P. Stoica, and A. Nehorai, "Maximum likelihood techniques for parameter estimation," in *Radar Array Processing*. New York: Springer-Verlag, 1993, ch. 4.
[7] L. Tong and S. Perreau, "Multichannel blind identification: From subspace methods to maximum likelihood methods," *Proc. IEEE*, vol. 86, no. 10, pp. 1951–1968, Oct. 1998.
[8] H. H. Zeng and L. Tong, "Blind channel estimation using the second-order statistics: Algorithms," *IEEE Trans. Signal Process.*, vol. 45, no. 8, pp. 1919–1930, Aug. 1997.
[9] Z. Xu, "Asymptotically near-optimal blind estimation of multipath CDMA channels," *IEEE Trans. Signal Process.*, vol. 49, no. 9, pp. 2003–2017, Sep. 2001.
[10] G. B. Giannakis and S. D. Halford, "Asymptotically optimal blind fractionally spaced channel estimation and performance analysis," *IEEE Trans. Signal Process.*, vol. 45, no. 7, pp. 1815–1830, Jul. 1997.
[11] H. H. Zeng and L. Tong, "Blind channel estimation using the second-order statistics: Asymptotic performance and limitations," *IEEE Trans. Signal Process.*, vol. 45, no. 8, pp. 2060–2071, Aug. 1997.
[12] P. Loubaton, E. Moulines, and P. Regalia, "Subspace method for blind identification and deconvolution," in *Signal Processing Advances in Wireless and Mobile Communications*. Englewood Cliffs, NJ: Prentice-Hall, 2000, vol. 1, ch. 3.
[13] P. Djuric, "Asymptotic MAP criteria for model selection," *IEEE Trans. Signal Process.*, vol. 46, no. 10, pp. 2726–2735, Oct. 1998.

Outage and Diversity of Linear Receivers in Flat-Fading MIMO Channels

Ahmadreza Hedayat, *Member, IEEE*, and
Aria Nosratinia, *Senior Member, IEEE*

***Abstract*—This correspondence studies linear receivers for multiple-input–multiple-output (MIMO) channels under frequency-nonselective (flat) quasi-static Rayleigh fading. The outage probability and diversity gain of minimum mean square error (MMSE) and zero forcing (ZF) receivers are investigated. Assuming M transmit and N receive antennas, the ZF receiver always has diversity $N - M + 1$, unlike the MMSE receiver which may exhibit a rate-dependent behavior. Under separate spatial encoding, where the parallel data streams are not jointly encoded, MMSE is no better than ZF in terms of diversity. Under joint spatial encoding, the MMSE receiver achieves diversity MN at low spectral efficiencies but has diversity only $M - N + 1$ at high spectral efficiencies. These results are established via simulations and an outline for the corresponding analysis is presented.**

***Index Terms*—Diversity, equalization, minimum mean square error (MMSE), multiple-input–multiple-output (MIMO), zero forcing (ZF).**

I. Introduction

In rich scattering conditions, multiple-input–multiple-output (MIMO) wireless channels can support high data rates through spatial multiplexing. Optimal reception, when complexity is not a concern, is through nonlinear nulling-and-cancelling [1]–[3], but when complexity is an issue one may use linear receivers. In this correspondence,

Manuscript received March 15, 2006. The associate editor coordinating the review of this manuscript and approving it for publication was Dr. Luc Vandendorpe. This work was presented in part at the International Conference on Acoustics, Speech, and Signal Processing, 2005.

A. Hedayat is with Navini Networks, Richardson, TX 75083 USA (e-mail: hedayat@ieee.org).

A. Nosratinia is with the Department of Electrical Engineering—MS 33, The University of Texas at Dallas, Richardson, TX 75083 USA (e-mail: aria@utdallas.edu).

Color versions of one or more of the figures in this paper are available online at http://ieeexplore.ieee.org.

Digital Object Identifier 10.1109/TSP.2007.901134

we study the outage[1] and diversity of linear MIMO receivers under quasi-static flat fading.

For a MIMO system consisting of M transmit and N receive antennas, under flat Rayleigh fading, simulations show that zero forcing (ZF) receivers achieve diversity order $M - N + 1$ under all cases studied. MMSE receivers achieve the same diversity *for transmission strategies that do not allow combined coding of data streams,* e.g., horizontal spatial encoding. However, for coding strategies that allow joint encoding of data streams, e.g., D-BLAST, a more interesting scenario emerges. In such systems, for low spectral efficiencies MMSE receivers can achieve the full diversity of MN, while for high spectral efficiencies only a diversity of $M + N - 1$ is possible. An outline for the analysis of the above results is presented. The ZF and MMSE analyses each use a conjecture whose rigorous demonstration remains open.

II. Linear Receivers

The input-output system model for flat fading MIMO channel with M transmit and $N \geq M$ receive antennas is $\mathbf{r} = \mathbf{Hc} + \mathbf{n}$, where $\mathbf{c}$ is the $M \times 1$ transmitted vector, $\mathbf{n} \in \mathcal{C}^{N\times 1}$ is the Gaussian noise vector, and $\mathbf{r}$ is the $N \times 1$ received vector at a given time instant. Throughout this correspondence, we assume $\mathbf{H}$ has independent and identically distributed complex Gaussian entries, i.e., $\mathbf{H} \in \mathcal{C}^{N\times M}$.

We evaluate the outage probability of a flat fading MIMO channel followed by a ZF or MMSE linear receiver, assuming the channel is perfectly known to the receiver. The ZF receiver is $\mathbf{F}_{\mathrm{ZF}} = (\mathbf{H}^H\mathbf{H})^{-1}\mathbf{H}^H$, which transforms the received signal-to-noise ratio (SNR)

$$\hat{\mathbf{r}} = \mathbf{F}_{\mathrm{ZF}}\mathbf{r} = \mathbf{c} + (\mathbf{H}^H\mathbf{H})^{-1}\mathbf{H}^H\mathbf{n}.$$

The MMSE receiver is $\mathbf{F}_{\mathrm{MMSE}} = (\mathbf{H}^H\mathbf{H} + \rho^{-1}\mathbf{I})^{-1}\mathbf{H}^H$, where ρ is the received SNR.

Since the symbols are detected individually, the SINR of the individual symbols determines the performance. The detection noise of ZF receiver $\tilde{\mathbf{n}} \triangleq (\mathbf{H}^H\mathbf{H})^{-1}\mathbf{H}^H\mathbf{n}$ is a complex Gaussian vector with zero-mean and covariance matrix $\mathbf{R}_{\tilde{\mathbf{n}}} = \sigma_n^2(\mathbf{H}^H\mathbf{H})^{-1}$. The removal of the kth row of $\mathbf{H}$ results in a new matrix denoted with $\hat{\mathbf{H}}$. Using this notation, the kth diagonal element of $\mathbf{R}_{\tilde{\mathbf{n}}}$ is given by

$$\mathbf{R}_{\tilde{\mathbf{n}}}(k,k) = \sigma_n^2(\mathbf{H}^H\mathbf{H})_k^{-1} = \sigma_n^2\frac{\det\left(\hat{\mathbf{H}}^H\hat{\mathbf{H}}\right)}{\det(\mathbf{H}^H\mathbf{H})} \tag{1}$$

where $(\mathbf{H}^H\mathbf{H})_k^{-1}$ represents the kth diagonal element of the inverse of $\mathbf{H}^H\mathbf{H}$. The SINR of kth equalized symbol is $\gamma_k = \mathcal{E}_x/\mathbf{R}_{\tilde{\mathbf{n}}}(k,k)$, which can be shown to be a chi-square random variable with $2(N - M + 1)$ degrees-of-freedom [4], [5]. The CDF of $Y \sim \chi_{2(N-M+1)}$, with variance 0.5 for the participating Gaussian random variables, is

$$F_Y(y) = 1 - e^{-y}\sum_{i=1}^{N-M+1}\frac{y^{i-1}}{(i-1)!}. \tag{2}$$

The SINR of the kth symbol of MMSE detector is determined by noise and residual interference

$$\gamma_k = \mathbf{h}_k^H\left(\hat{\mathbf{H}}_k\hat{\mathbf{H}}_k^H + \rho^{-1}\mathbf{I}\right)^{-1}\mathbf{h}_k \tag{3}$$

$$= \frac{1}{(\mathbf{I} + \rho\mathbf{H}^H\mathbf{H})_k^{-1}} - 1 \tag{4}$$

where $\mathbf{h}_k$ is the kth column of $\mathbf{H}$. Removing this column from $\mathbf{H}$ gives $\hat{\mathbf{H}}_k \in \mathcal{C}^{N\times(M-1)}$[6].

[1]For good codes and long block lengths, outage probability gives an approximation of the frame error rate.

Equation (4) shows that γ_k is a quadratic form whose statistics has been derived in [7] as follows. Considering the random matrix $\hat{\mathbf{H}} \in \mathcal{C}^{N\times(M-1)}$ and the random vector $\mathbf{h} \in \mathcal{C}^N$, the quadratic form $Y = \mathbf{h}^H(\hat{\mathbf{H}}\hat{\mathbf{H}}^H + \rho^{-1}\mathbf{I})^{-1}\mathbf{h}$ has the CDF

$$F_Y(y) = 1 - \exp\left(-\frac{y}{\rho}\right)\sum_{n=1}^{N}\frac{A_n(y)}{(n-1)!}\left(\frac{y}{\rho}\right)^{n-1} \tag{5}$$

where the auxiliary functions $A_n(y)$ are given by

$$A_n(y) = \begin{cases} 1 & N \geq M + n - 1 \\ \frac{1+\sum_{i=1}^{N-n} C_i y^i}{(1+y)^{M-1}} & N < M + n - 1 \end{cases} \tag{6}$$

and C_i is the coefficient of y^i in $(1+y)^{M-1}$[7]. In general, the SINR of the output symbols of the ZF and MMSE receivers are correlated.

III. Outage Probability in Separate Spatial Encoding

In separate spatial encoding, the data stream is demultiplexed to several substreams, each separately encoded and fed to the corresponding antenna. Horizontally encoded V-BLAST is a prominent example of this strategy. In this scenario, if any of the data streams is in outage, the entire system is in outage. Hence, the outage event $\mathcal{O}$ occurs when any of the subchannels cannot support the rate that is assigned to it. In our analysis, we consider equal rate for the subchannels. Generalization to nonuniform rate assignment is immediate, since uniform and nonuniform rate assignments have the same diversity.

At the output of the linear receiver, the mutual information between the elements of $\hat{\mathbf{r}}$ and the transmitted data vector $\mathbf{c}$ is $\mathcal{I}(c_k;\hat{r}_k) = \log(1+\gamma_k)$. Assume the target rate is R and let $L \triangleq N - M$. According to (2) and (5), the statistics of γ_k is invariant to k. Thus, the outage probability $\Pr(\mathcal{O})$ is

$$\begin{aligned}\Pr(\mathcal{O}) &= 1 - \Pr\left(\bigcap_{k=1}^{M}\left\{\mathcal{I}(c_k;\hat{r}_k) \geq \frac{R}{M}\right\}\right)\\ &= 1 - \left(\Pr\left(\mathcal{I}(c_k;\hat{r}_k) \geq \frac{R}{M}\right)\right)^M\\ &\approx M\Pr\left(\mathcal{I}(c_k;\hat{r}_k) < \frac{R}{M}\right)\end{aligned} \tag{7}$$

where (7) is accurate when subchannel outage probabilities are small. In (7), we have assumed that subchannel outage events are independent. In linear receivers the subchannel outage events are not strictly independent, but the approximation makes the analysis tractable and does not affect diversity, as verified by simulations. Alternatively, one may consider only the outage event of a single subchannel, which is an approximation that is accurate enough for diversity calculation.

Using the CDF of $\chi_{2(N-M+1)}$ in the evaluation of (7) gives the outage probability for the ZF receiver, which is

$$\begin{aligned}\Pr(\mathcal{O}) &\approx MF_Y(2^{R/M} - 1)\\ &\mathrel{\dot{=}} \frac{M(2^{R/M}-1)^{L+1}}{(L+1)!}\rho^{-(L+1)}\end{aligned} \tag{8}$$

where $\mathrel{\dot{=}}$ denotes equivalence in the limit as $\rho \to \infty$. Thus, the ZF diversity order is $L + 1$. Substituting the distribution (5) in (7), the MMSE outage probability is calculated

$$\begin{aligned}\Pr(\mathcal{O}) &\approx MF_Y(2^{R/M} - 1)\\ &\mathrel{\dot{=}} \frac{y^{L+1}}{(L+1)!}\cdot\frac{y^{M-1}}{(1+y)^{M-1}}\rho^{-(L+1)}\Bigg|_{y=2^{R/M}-1}\end{aligned} \tag{9}$$

which shows that MMSE diversity order is also $L+1$. However, the ZF and MMSE outage probabilities are not exactly the same. The ratio of (8) to (9) is

$$\frac{\Pr(\mathcal{O})_{ZF}}{\Pr(\mathcal{O})_{\mathrm{MMSE}}} = \left.\frac{(1+y)^{M-1}}{y^{M-1}}\right|_{y=2^{R/M}-1} = \left(\frac{2^{R/M}}{2^{R/M}-1}\right)^{M-1}. \tag{10}$$

Note that the ratio of outage probabilities in (10) is independent of SNR and is only a function of the relative target rate R/M. When R/M is small the outage probability of ZF is larger than MMSE. The ratio (10) approaches unity when R/M is large (see Section V).

IV. Outage Probability in Joint Spatial Encoding

In joint spatial encoding, the data stream is encoded and then demultiplexed into substreams, each going to one antenna (e.g., D-BLAST). Thus, each data symbol can contribute to signals of all the transmit antennas. The receiver is in outage when the aggregate mutual information of all the subchannels fails to support the target rate.

Assuming the target rate is R, the probability of the outage event $\mathcal{O}$ is

$$\Pr(\mathcal{O}) = \Pr\left(\sum_{k=1}^{M}\log(1+\gamma_k) < R\right) \tag{11}$$

$$= \Pr\left(\prod_{k=1}^{M}(1+\gamma_k) < 2^R\right). \tag{12}$$

The SINR of the subchannels γ_k under ZF are identically distributed (but not independent) chi-square random variables with degrees $2(N-M+1)$. Intuitively, the diversity arising from coding across channels with independent power levels is no worse than coding across channels whose power levels are random and correlated. Subject to this conjecture, we have the following.

Theorem 1: Consider a flat MIMO channel with M transmit and $N \geq M$ receive antennas and joint spatial encoding. Under perfect channel state information available to the receiver, the ZF receiver has diversity no better than $N-M+1$.

Proof: See the Appendix. ■

Since the diversity of joint spatial encoding is lower bounded by diversity of separate spatial encoding, we conclude that ZF diversity must be the same for both. This result is verified by simulations.

To obtain the MMSE outage probability, we substitute the SINR from (4) in (12), which gives

$$\Pr(\mathcal{O}) = \Pr\left(\prod_{k=1}^{M}(\mathbf{I}+\rho\mathbf{H}^H\mathbf{H})_k^{-1} > 2^{-R}\right). \tag{13}$$

The dependence on the diagonal elements of the random matrix $(\mathbf{I}+\rho\mathbf{H}^H\mathbf{H})^{-1}$ makes further analysis intractable. Therefore, we proceed to provide an upper bound to this probability. Rewriting the sum mutual information as in (11), we have

$$-\sum_{k=1}^{M}\mathcal{I}(c_k;\hat{r}_k) = \sum_{k=1}^{M}\log\left((\mathbf{I}+\rho\mathbf{H}^H\mathbf{H})_k^{-1}\right)$$

$$\leq M\log\left(\sum_{k=1}^{M}\frac{1}{M}(\mathbf{I}+\rho\mathbf{H}^H\mathbf{H})_k^{-1}\right) \tag{14}$$

$$= M\log\left(\frac{1}{M}\mathrm{tr}\left((\mathbf{I}+\rho\mathbf{H}^H\mathbf{H})^{-1}\right)\right)$$

$$= M\log\left(\frac{1}{M}\sum_{k=1}^{M}\frac{1}{1+\rho\lambda_k}\right) \tag{15}$$

where (14) is due to Jensen's inequality and λ_k's are the eigenvalues of the Wishart matrix $\mathbf{H}^H\mathbf{H}$. Substituting (15) into (11) gives

$$\Pr(\mathcal{O}) \leq \Pr\left(\sum_{k=1}^{M}\frac{1}{1+\rho\lambda_k} \geq M2^{-R/M}\right). \tag{16}$$

This is an upper bound of the outage probability, which we conjecture to be tight. The tightness of this bound in both low and high spectral efficiency is demonstrated via simulations in Section V. In the sequel, we continue working with this bound, while noting that a rigorous proof of the tightness of this bound remains open for future work. Assuming $N \geq M$, the joint PDF of the eigenvalues of $\mathbf{H}^H\mathbf{H}$, λ_k's, $\lambda_1 \leq \lambda_2 \leq \cdots \leq \lambda_M$, is

$$f_{\mathbf{\Lambda}}(\boldsymbol{\lambda}) = K_{M,N}\prod_{i=1}^{M}\lambda_i^{N-M}\prod_{i<j}(\lambda_i-\lambda_j)^2\exp\left(-\sum_i\lambda_i\right) \tag{17}$$

where $K_{M,N}$ is a normalizing constant [8].

The evaluation of (16) for a specific outage rate R is rather difficult, due to the shape of the outage region. However, one can calculate the bound for small and large values of R where the outage region can be approximated by regions with simpler shapes.

For a MIMO channel with $M=2$ and $N \geq 2$, the bound (16) is

$$\Pr(\mathcal{O}) \leq \Pr\left(\frac{1}{1+\rho\lambda_1}+\frac{1}{1+\rho\lambda_2} \geq 2^{1-(R/2)}\right). \tag{18}$$

For convenience define $S(\lambda_1,\lambda_2) \triangleq 1/(1+\rho\lambda_1)+1/(1+\rho\lambda_2)$ and also define the set $\mathcal{A} \triangleq \left\{(\lambda_1,\lambda_2) : S(\lambda_1,\lambda_2) \geq 2^{1-(R/2)}\right\}$. Then the right-hand side of (18) is $\Pr(\mathcal{A})$. Exact calculation of $\Pr(\mathcal{A})$ is not easy, thus, we show its asymptotic behavior by bounding it from below and above.

Let $0 \leq R < 2$. If $\lambda_1 = 0$ outage occurs only when $\lambda_2 \leq c_2 \triangleq (2-b)/(\rho(b-1))$, where $b \triangleq 2^{1-R/2}$. Because the curve $S(\lambda_1,\lambda_2) = b$ is convex, the region $\mathcal{A}$ is contained in the isosceles right triangle with the base $\lambda_1+\lambda_2 = c_2$ and the two sides $\lambda_1 = 0$ and $\lambda_2 = 0$, and integral over the triangle is always larger than $\Pr(\mathcal{A})$.

We now build another triangle that is *contained* by $\mathcal{A}$. Using the symmetry of $S(\lambda_1,\lambda_2)$, it is not difficult to calculate that an isosceles triangle with base $\lambda_1+\lambda_2 = \tilde{c}_2$, where $\tilde{c}_2 = (2-b)/b\rho$, is contained in $\mathcal{A}$ and integration over this triangle is always smaller than $\Pr(\mathcal{A})$.

Finally, we show that probability integrals over the two triangles behave the same asymptotically, thus completing a sandwich argument. To do so, consider the integral over any such isosceles triangle with parameter c

$$K_{2,N}\int_0^c e^{-\lambda_1}\lambda_1^{N-2}\int_0^{c-\lambda_1}\lambda_2^{N-2}(\lambda_1-\lambda_2)^2e^{-\lambda_2}d\lambda_2 d\lambda_1$$

$$= 2K_{2,N}(N-1)!(N-2)!\left(1-e^{-c}\sum_{k=1}^{2N-1}\frac{c^k}{k!}\right)$$

$$\mathrel{\dot{=}} \rho^{-2N} \tag{19}$$

where c could be c_2 or $\tilde{c}_2$. Since $\Pr(\mathcal{A})$ is bounded above and below by values that have diversity-$2N$, it must have diversity $2N$. Now recall that $\Pr(\mathcal{O}) \leq \Pr(\mathcal{A})$, therefore, we have established that outage has diversity no less than $2N$. Considering that $2N$ is also the maximum achievable diversity order, we conclude that outage has exactly diversity order $2N$. This concludes the arguments for small spectral efficiencies.

Now we consider high spectral efficiencies, namely $R > 2$ and $0 \leq b < 1$. In this case, λ_2 can drive the system to outage regardless of the value of λ_1 (and vice versa). For instance, let $\lambda_1 \to \infty$, as long as $\lambda_2 \leq d_2 = (1-b/\rho b)$, outage occurs. Thus, the outage region includes a strip along the λ_1 axis for large enough λ_1, and likewise along λ_2. In fact, the set of strips defined as $0 \leq \lambda_2, 0 \leq \lambda_1 \leq d_2$, and

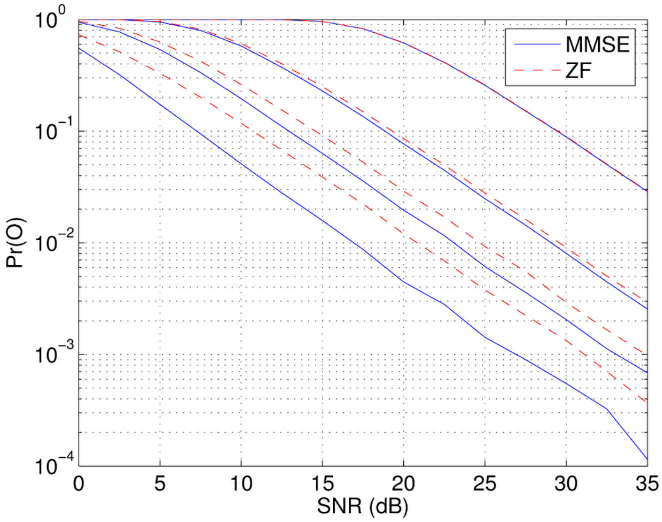

Fig. 1. Outage probability of linear receivers, $M = N = 2$. The pairs of solid and dashed lines, from left, correspond to MMSE and ZF for rates $R = 1, 2, 4, 10$ bits/s/Hz.

$0 \le \lambda_1, 0 \le \lambda_2 \le d_2$ is contained in $\mathcal{A}$, and the set of strips $0 \le \lambda_2$, $0 \le \lambda_1 \le \tilde{d}_2$, and $0 \le \lambda_1, 0 \le \lambda_2 \le \tilde{d}_2$, where $\tilde{d}_2 = 2 - b/\rho b$ contains $\mathcal{A}$. The probability of the previous sets can be characterized using the following expression:

$$2K_{2,N}\int_0^d e^{-\lambda_1}\lambda_1^{N-2}\int_0^\infty \lambda_2^{N-2}(\lambda_1-\lambda_2)^2 e^{-\lambda_2}d\lambda_2 d\lambda_1 \doteq \rho^{-(N-1)} \tag{20}$$

where d could be d_2 or $\tilde{d}_2$. Therefore, (20) indicates that the upper bound (18) has the diversity $N-1 = L+1$, where $L = N - M$. In the calculation of (20), the intersection of the two orthogonal strips is calculated twice, but the intersection has a probability that decays with $\rho^{-2(N-1)}$ and does not affect the asymptotic behavior of (20).

The outage bounds suggest that MMSE receivers can achieve the same diversity as the ML receiver for small values of R in joint spatial encoding. However, for large values of R the diversity performance of MMSE and ZF is the same.

The previous results for the case $M = 2, N \ge 2$ can be extended to arbitrary values of M and $N \ge M$. We state the general result in the following theorem.

Theorem 2: Consider a flat MIMO channel with M transmit and $N \ge M$ receive antennas, and joint spatial encoding. Under perfect channel state information available to the receiver, the upper bound (16) on the outage probability of MMSE receivers decays with order of MN at low spectral efficiency, i.e., $R < M\log(M/(M-1))$, resulting in the diversity order of MN for the outage probability. At high spectral efficiency $R > M\log M$, (16) decays with the order of $N - M + 1$.

Proof: See the Appendix. ■

V. Simulation Results

We consider a MIMO system with two antennas in transmit and receive sides: $M = N = 2$. The outage probability of the linear receivers in the separate architecture is shown in Fig. 1. The target rate is $R = 1, 2, 4, 10$ bits/s/Hz. As expected, both linear detectors show diversity order of one, regardless of the target rate. For higher values of R the difference of ZF and MMSE performance is negligible. But for lower values of R, MMSE performs better than ZF for all SNR. The dependency of the relative performance of these receivers on the target rate R is in agreement with (10). In high SNR, the ratio of the outage probabilities remains fixed.

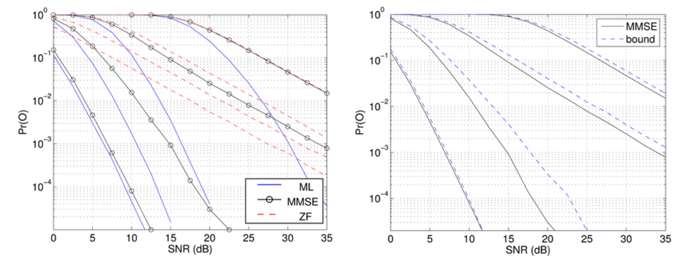

Fig. 2. (Left) Comparison of receivers. (Right) MMSE outage and the upper bound (16). $M = N = 2$ and the curves show rates $R = 1, 2, 4, 10$ bits/s/Hz.

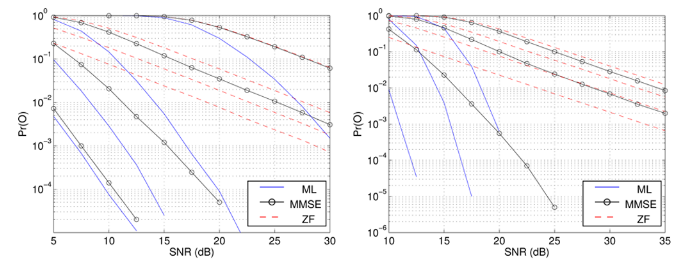

Fig. 3. Comparison of receivers. (Left) $M = N = 2$, correlated transmit antennas with $\rho_t = 0.5$, $R = 1, 2, 4, 10$ bits/s/Hz. (Right) $M = N = 4$, uncorrelated, $R = 4, 8, 12, 16$ bits/s/Hz.

Fig. 2 shows the outage probability of an optimal (nonlinear) receiver as well as linear receivers, in a joint spatial encoding architecture. Naturally the optimal receiver has the full diversity of the channel. We see the diversity order of ZF is independent of the target rate R, but MMSE diversity depends on R: at lower values of R the diversity order is very close to that of the optimal receiver, while at higher values of R its diversity is equal to ZF diversity.

Fig. 2 also shows the outage probability of the MMSE receiver and the upper bound (16). The bound is tight at either low or high values of R. The bound is not tight at intermediate values of R, but its slope still shows the diversity order.

Fig. 3 presents similar results for a flat fading MIMO channel with $M = N = 2$ and correlated transmit antennas with correlation factor $\rho_t = 0.5$. Outage probabilities are slightly higher than the uncorrelated case, but the diversity is unchanged. Fig. 3 also shows the results for uncorrelated MIMO channel with $M = N = 4$.

VI. Conclusion

We study the diversity of linear receivers for MIMO Rayleigh flat fading channels. We find that while ZF receivers have a fixed diversity of $N - M + 1$ under all conditions, MMSE receivers have a diversity that may vary between $N - M + 1$ and NM, depending on spectral efficiency and the manner of the encoding of data streams. The ZF and MMSE analyses each use a conjecture whose rigorous demonstration remains an open problem.

Appendix

Proof of Theorem 1: Recalling the conjecture mentioned earlier, we assume the SINR of the subchannels are independent chi-square random variables with degrees $2(N-M+1)$. Let $Y_k \sim \chi_{2(N-M+1)}$, $k = 1, \ldots, M$. The outage probability of ZF is given by the CDF of

$$\prod_{k=1}^{M}(1+Y_k) = 1 + \sum_{k=1}^{M} Y_k + \cdots + \prod_{k=1}^{M} Y_k. \tag{21}$$

The last term, which is the product of Y_k's, determines the diversity order since it is a chi-square with the lowest degree. In the following, through recursion, we show that $Y_1 \cdot Y_2, \ldots, Y_M$ has diversity order $L+1$. Let us start by $Z \triangleq Y_1 \cdot Y_2$. The PDF of Z is

$$f_Z(z) = \frac{2}{((L-1)!)^2} z^L K_0(2\sqrt{z}) \tag{22}$$

where $K_0(\cdot)$ is the zeroth-order modified Bessel function of the second kind [9], which for small values of z is a constant.[2] Therefore, for small values of z the first-order approximation of $f_Z(z)$ is z^L. This shows that the CDF of Z, $F_Z(z)$, has first order approximation equal to z^{L+1}, which indicates the diversity order of $L+1$. Now consider the CDF of $W \triangleq Y_1 \cdot Y_2 \cdot Y_3 = Z \cdot Y$, where $Y \sim \chi_{2(N-M+1)}$

$$\begin{aligned} F_W(w) &= \Pr(W \le w) = \Pr(Z \cdot Y \le w) \\ &= \int_0^\infty f_Z(z) F_Y\left(\frac{w}{z}\right) dz \\ &= \alpha \int_0^\infty z^L K_0(2\sqrt{z}) e^{-w/z} \sum_{k=L+2}^{\infty} \frac{w^{k-1}}{z^{k-1}(k-1)!} dz \end{aligned}$$

where α is a constant. The first-order approximation of above around zero is

$$w^{L+1} \int_0^\infty \frac{\alpha}{z(L+1)!} K_0(2\sqrt{z}) dz.$$

Thus, $F_W(w)$ behaves like w^{L+1}. By recursion one finds that first-order approximation of $F_{Y_1 \cdot Y_2, \ldots, Y_M}$ behaves like w^{L+1}, so it has diversity $L+1$. As mentioned earlier, the product term dominates in (21), therefore, the ZF diversity order is $L+1$. ■

Proof of Theorem 2: First, we state and prove the following lemma.

Lemma 1: Let

$$I_M = \int \cdots \int_{\sum_i \lambda_i \le x} e^{-\sum_i \lambda_i} \prod_{i=1}^{M} \lambda_i^{k_i} d\lambda_1 \cdots d\lambda_M. \tag{23}$$

I_M is polynomial in x with the minimum exponent of $g(M) = M + \sum_{i=1}^{M} k_i$, where M and k_i are integers.

Proof: With some algebra, one can obtain

$$\int_0^x \lambda^m e^{-\lambda} d\lambda = m! \sum_{i=m+1}^{\infty} \frac{x^i}{i!}, \tag{24}$$

$$\begin{aligned} \int_0^x \lambda^m (x-\lambda)^n e^{-\lambda} d\lambda &= \sum_{j=0}^{n} C(j,n)(-1)^j x^{n-j} (m+j)! \\ &\quad \times \sum_{\ell=m+j+1}^{\infty} \frac{x^\ell}{\ell!} \end{aligned} \tag{25}$$

where m and n are integers and $C(\cdot,\cdot)$ are the binomial coefficients. Using (24) and (25), I_2 can be calculated as

$$I_2 = \sum_{i=k_1+1}^{\infty} \frac{n!}{i!} \sum_{j=0}^{i} C(j,i)(-1)^j x^{i-j} (k_2+j)! \sum_{\ell=k_2+j+1}^{\infty} \frac{x^\ell}{\ell!}$$

where the minimum exponent of x is $g(2) = k_1 + k_2 + 2$.

[2]For small values of x: $K_m(x) \sim (\Gamma(m)/2)(2/x)^m$[9].

Now we use induction. Assume that $I_{M-1} = \sum_{i=g(M-1)}^{\infty} a_i x^i$. Then

$$\begin{aligned} I_M &= \int_0^x \lambda_M^{k_M} e^{-\lambda_M} \int \cdots \int_{\sum_i^{M-1} \lambda_i \le x - \lambda_M} e^{-\sum_i^{M-1} \lambda_i} \\ &\quad \times \prod_{i=1}^{M-1} \lambda_i^{k_i} d\lambda_1 \cdots d\lambda_M \\ &= \sum_{i=g(M-1)}^{\infty} a_i \int_0^x \lambda_M^{k_M} e^{-\lambda_M} (x-\lambda_M)^i d\lambda_M \\ &= \sum_{i=g(M-1)}^{\infty} a_i \sum_{j=0}^{i} C(j,i)(-1)^j x^{i-j} (k_M+j)! \\ &\quad \times \sum_{\ell=k_M+j+1}^{\infty} \frac{x^\ell}{\ell!} \end{aligned} \tag{26}$$

where (26) is obtained using (25). Equation (26) indicates that I_M is polynomial in x with the minimum exponent of $g(M-1) + k_M + 1 = g(M)$. ■

To prove Theorem 2, we first note that

$$\prod_{i<j} (\lambda_i - \lambda_j)^2 = \sum_{(k_1,\ldots,k_M) \in \mathcal{S}} p(k_1, \ldots, k_M) \prod_{i=1}^{M} \lambda_i^{k_i} \tag{27}$$

where the set $\mathcal{S}$ is a subset of the $(k_1, \ldots, k_M)$ indexes that $\sum_{i=1}^{M} k_i = M(M-1)$, and $p(k_1, \ldots, k_M)$ is the corresponding integer coefficient.

In low spectral efficiency $R < M \log(M/(M-1))$, we can write the right-hand side of (16) as

$$\begin{aligned} &K_{M,N} \int \cdots \int_{\mathcal{A}} e^{-\sum_i \lambda_i} \prod_{i=1}^{M} \lambda_i^{N-M} \prod_{i<j} (\lambda_i - \lambda_j)^2 d\lambda_1 \cdots d\lambda_M \\ &= K_{M,N} \sum_{(k_1,\ldots,k_M) \in \mathcal{S}} p(k_1, \ldots, k_M) \\ &\quad \times \int \cdots \int_{\mathcal{A}} e^{-\sum_i \lambda_i} \prod_{i=1}^{M} \lambda_i^{N-M+k_i} d\lambda_1 \cdots d\lambda_M. \end{aligned} \tag{28}$$

We now bound the integration region $\mathcal{A}$, from inside and from outside, by polyhedra. Then we use a sandwich argument by showing that the integration over the inner and outer polyhedra gives the same asymptotic performance.

Using a direct extension of the argument developed in the 2-D case [proceeding (19)], it can be seen that the polyhedron defined by $\lambda_i \ge 0, \sum_i \lambda_i \le c_M$, where

$$c_M = \rho^{-1} \frac{M(1 - 2^{-R/M})}{1 + M(2^{-R/M} - 1)}$$

contains the integration region $\mathcal{A}$. Therefore an integral over this polyhedron upper bounds the outage probability.

Now consider another polyhedron defined by $\lambda_i \ge 0, \sum_i \lambda_i \le \tilde{c}_M$, where $\tilde{c}_M$ is proportional to ρ^{-1} but small enough so that $\mathcal{A}$ contains this polyhedron. The base of this polyhedron can be calculated in a manner similar to Section IV

$$\tilde{c}_M = \rho^{-1}(2^{R/M} - 1).$$

Integration over this new polyhedron, which is characterized by $\tilde{c}_M$, lower bounds $\Pr(\mathcal{A})$.

Finally, Lemma 1 establishes that the asymptotic behavior of (28), while integrating over either of the two polyhedra, is the same. Each multiple integral in (28) is in the form of I_M of Lemma 1, i.e., polynomial in c_M with smallest exponent $M+\sum_{i=1}^{M}(N-M+k_i)=MN$. Therefore, the upper bound (16) decays with ρ^{-MN} in low spectral efficiency, indicating diversity order is no less than MN. At the same time, MN is actually the maximum possible diversity order, so the outage probability of MMSE receiver has diversity of MN.

We now proceed to show the high-rate result, where the developments parallel those for $M=2$ in (20). For $R>M\log M$ the outage region $\mathcal{A}$ can be upper and lower bounded with orthogonal slabs along the coordinates. The first set that is a subset of $\mathcal{A}$ has M orthogonal slabs where the jth slab is defined as $\lambda_j \le d_M$ and $\lambda_{i\neq j}\ge 0$, where $d_M=\rho^{-1}((1/M)2^{R/M}-1)$. The outage region $\mathcal{A}$ is a subset of the second set of slabs whose definition is the same as the first set with d_M replaced with $\tilde{d}_M=\rho^{-1}(2^{R/M}-1)$.

Therefore, the right-hand side of the bound (16) is the same as (28) with the exception that the integration region $\mathcal{A}$ could be either of above sets. Considering the possibility of some zero k_i in (27) and the unbounded shape of $\mathcal{A}$, there are dominating terms such as

$$\int\cdots\int_{\lambda_j\le d_M,\lambda_{i\neq j}\ge 0} e^{-\sum_i \lambda_i}\lambda_j^{N-M}\times\prod_{i\neq j}^{M}\lambda_i^{N-M+k_i}d\lambda_1\cdots d\lambda_M$$

which is polynomial in d_M with the minimum exponent of $N-M+1$. This indicates that the bound (16) decays with $\rho^{-(N-M+1)}$ in high spectral efficiency. This completes the proof of Theorem 2. ∎

ACKNOWLEDGMENT

The authors would like to thank Dr. G. Caire and Dr. N. Al-Dhahir for their comments.

REFERENCES

[1] G. Foschini, G. Golden, R. Valenzuela, and P. Wolniansky, "Simplified processing for high spectral efficiency wireless communication employing multi-element arrays," *J. Sel. Areas Commun.*, vol. 17, pp. 1841–1852, Nov. 1999.

[2] N. Prasad and M. K. Varanasi, "Outage analysis and optimization for multiaccess and V-BLAST architecture over MIMO Rayleigh fading channels," in *Proc. 41th Ann. Allerton Conf. Commun., Control, Comput.*, 2003, pp. 358–367.

[3] T. Guess, H. Zhang, and T. V. Kotchiev, "The outage capacity of BLAST for MIMO channels," in *Proc. IEEE ICC*, 2003, pp. 2628–2632.

[4] J. H. Winters, J. Salz, and R. D. Gitlin, "The impact of antenna diversity on the capacity of wireless communication systems," *IEEE Trans. Commun.*, vol. 43, no. 1, pp. 1740–1750, Feb./Mar./Apr. 1994.

[5] M. Rupp, C. Mecklenbrauker, and G. Gritsch, "High diversity with simple space time block-codes and linear receivers," in *Proc. IEEE GLOBECOM*, 2003, pp. 302–306.

[6] E. K. Onggosanusi, A. G. Dabak, T. Schmidl, and T. Muharemovic, "Capacity analysis of frequency-selective MIMO channels with suboptimal detectors," in *Proc. IEEE ICASSP*, 2002, pp. 2369–2372.

[7] H. Gao, P. J. Smith, and M. V. Clark, "Theoretical reliability of MMSE linear diversity combining in Rayleigh-fading additive interference channels," *IEEE Trans. Commun.*, vol. 46, no. 5, pp. 666–672, May 1998.

[8] L. Zheng and D. Tse, "Diversity and multiplexing: A fundamental tradeoff in multiple-antenna channels," *IEEE Trans. Inf. Theory*, vol. 49, no. 5, pp. 1073–1096, May 2003.

[9] I. S. Gradshteyn and I. M. Ryzhik, *Table of Integrals, Series, and Products*, 5th ed. San Diego, CA: Academic, 1994.

Joint MIMO Channel Tracking and Symbol Decoding Using Kalman Filtering

B. Balakumar, S. Shahbazpanahi, and T. Kirubarajan

***Abstract*—In this paper, the problem of channel tracking is considered for multiple-input multiple-output (MIMO) communication systems where the MIMO channel is time-varying. We consider a class of MIMO systems where orthogonal space–time block codes are used as the underlying space–time coding schemes. For such systems, a two-step MIMO channel tracking algorithm is proposed. As the first step, Kalman filtering is used to obtain an initial channel estimate for the current block based on the channel estimates obtained for previous blocks. Then, in the second step, the so-obtained initial channel estimate is refined using a decision-directed iterative method. We show that, due to specific properties of orthogonal space–time block codes, both the Kalman filter and the decision-directed algorithm can be significantly simplified. Simulation results show that the proposed tracking method can provide results in a symbol error rate performance that is 1 dB better than that of the differential receiver.**

***Index Terms*—Channel tracking, decision-directed channel equalization, Kalman filtering, multiple-input multiple-output (MIMO) communications, space–time coding.**

I. INTRODUCTION

Multiple-input multiple-output (MIMO) communications and space–time coding have been the focus of extensive research efforts. Among different space–time coding schemes presented in the literature, orthogonal space–time block codes (OSTBCs) [1], [2] are of particular interest because they achieve full diversity at a low receiver complexity. Indeed, given the MIMO channel, the maximum likelihood (ML) optimal receiver for OSTBCs consists of a linear receiver followed by a symbol-by-symbol decoder. Also, it has recently been shown in [3] that for a majority of OSTBCs, the MIMO channel is blindly identifiable. This interesting property of OSTBCs is based on the assumption that the channel is fixed during a long enough time interval. However, the channel may be time-varying in practice due to the mobility of the transmitter and/or receiver, as well as due to the carrier frequency mismatch between the transmitter and receiver. Therefore, channel tracking is essential in these cases.

In [4], Kalman filtering has been studied in application to channel tracking for MIMO communication systems. The method of [4] is based on two assumptions. First, the underlying space–time coding scheme is based on Alamouti code [1], and therefore its application is limited to the case of two transmit antennas. Second, the channel is assumed to be time-varying during the transmission of each block. The latter assumption implies that the linear ML receiver is optimal in a mean sense [4].

Kalman filtering has been applied to the problem of MIMO channel tracking in several other research reports [5], [6]. Also, in [7], a fre-

Manuscript received September 19, 2006; revised April 27, 2007. The associate editor coordinating the review of this manuscript and approving it for publication was Prof. Simon J. Godsill.This paper was presented in parts at the 2006 IEEE Workshop on Sensor Array and Multichannel Signal Processing (IEEE SAM'06), Waltham, MA, and the 2006 European Signal Processing Conference (EUSIPCO'06), Florence, Italy.

B. Balakumar and T. Kirubarajan are with the Department of Electrical and Computer Engineering, McMaster University, Hamilton, ON L8S 4K1, Canada (e-mail: bala@grads.ece.mcmaster.ca; kiruba@mcmaster.ca).

S. Shahbazpanahi is with the Faculty of Engineering and Applied Science, University of Ontario Institute of Technology, Oshawa, ON L1H 7K4, Canada (e-mail: shahram.shahbazpanahi@uoit.ca).

Digital Object Identifier 10.1109/TSP.2007.901663